Importance of the Fermi-surface topology to the superconducting state of the electron-doped pnictide Ba(Fe$_{1-x}$Co$_x$)$_2$As$_2$

Chang Liu, A. D. Palczewski, R. S. Dhaka, Takeshi Kondo, R. M. Fernandes, E. D. Mun, H. Hodovanets, A. N. Thaler, J. Schmalian, S. L. Bud'ko, P. C. Canfield, and A. Kaminski

Ames Laboratory and Department of Physics and Astronomy, Iowa State University, Ames, Iowa 50011, USA

We used angle-resolved photoemission spectroscopy and thermoelectric power to study the poorly explored, highly overdoped side of the phase diagram of Ba(Fe$_{1-x}$Co$_x$)$_2$As$_2$ high-temperature superconductor. Our data demonstrate that several Lifshitz transitions—topological changes of the Fermi surface—occur for large x. The central hole barrel changes to ellipsoids that are centered at Z at $x \sim 0.11$ and subsequently disappear around $x \sim 0.2$; changes in thermoelectric power occur at similar x values. T_c decreases and goes to zero around $x \sim 0.15$—between the two Lifshitz transitions. Beyond $x = 0.2$ the central pocket becomes electron-like and superconductivity does not exist. Our observations reveal the importance of the underlying Fermiology in electron-doped iron arsenides. We speculate that a likely necessary condition for superconductivity in these materials is the presence of the central hole pockets rather than nesting between central and corner pockets.

The phase diagrams of the iron arsenic superconductors contain a number of intriguing features. For the electron-doped A(Fe$_{1-x}$T$_x$)$_2$As$_2$ series (122, A = Ca, Sr, Ba; T = Co, Ni, Pd, etc.), superconductivity is found in both regions with and without a long-range antiferromagnetic (AFM) order.[1–7] The superconducting (SC) region extends to different doping levels for different dopants, but scales very well if the horizontal axis of the phase diagram was chosen to be the number of extra electrons.[6,7] It is therefore likely that changes in the underlying electronic structure due to electron doping are linked closely to their SC behavior. On the underdoped side, a recent angle-resolved photoemission spectroscopy (ARPES) study on Ba(Fe$_{1-x}$Co$_x$)$_2$As$_2$ (Ref. 8) revealed that superconductivity emerges at a doping level (x_{on}) where a topological change of the Fermi surface (Lifshitz transition[9] at doping x_1) reduces the magnetically reconstructed Fermi surface to its paramagnetic appearance, i.e., $x_1 \simeq x_{\text{on}}$. This transition exhibits itself as a rapid change of Hall coefficient and thermoelectric power (TEP) in transport measurements.[10] An immediate question is whether a similar change of Fermiology causes the collapse of the SC dome on the heavily overdoped regime. It is inevitable that the hole pockets surrounding the central axis of the Brillouin zone (Γ-Z) will shrink in size and vanish at some higher doping x_2. The question is whether this Lifshitz transition correlates with the offset of superconductivity on the overdoped side of the phase diagram (x_{off}). Theoretically, Lifshitz transitions have been found to affect T_c greatly in multiband systems.[11] Fernandes and Schmalian[12] showed that for the electron-doped pnictides, the disappearance of superconductivity is directly linked to the vanishing of the central hole pocket(s), i.e., $x_2 \simeq x_{\text{off}}$. Experimentally, the Hall coefficient vs doping on Ba(Fe$_{1-x}$Co$_x$)$_2$As$_2$ (Ref. 4) experiences a slight change of slope around x_{off}, hinting at a possible Lifshitz transition close to the high doping offset of superconductivity.

In this Rapid Communication, we study this issue in detail using ARPES and TEP measurements. We performed a complete survey of the electronic structure on the overdoped part of the phase diagram of this material. This survey reveals that topological changes of the Fermi surface likely link to the suppression of superconductivity in electron-doped pnictides. In the overdoped side, the outer hole barrel surrounding the zone center (Γ-Z) changes to ellipsoids centering at Z at a doping of $x_{2\Gamma} \sim 0.11$. T_c is driven to zero before the disappearance of Z ellipsoids and the change in TEP at $x_{2Z} \sim 0.2$. In short, we find that $x_{2\Gamma} < x_{\text{off}} < x_{2Z}$. Our data demonstrated that superconductivity in the pnictides is very robust with respect to doping; the whole Γ Fermi sheet has to be almost completely eliminated in order to drive T_c to zero. A likely necessary condition for superconductivity then is the existence of the central hole pockets rather than a perfect nesting between the Γ and X pockets,[13] as is also the case in LiFeAs.[14] The dominant contribution to the pairing interaction is believed to come from interband coupling between the central and corner pockets.[12]

Single crystals of Ba(Fe$_{1-x}$Co$_x$)$_2$As$_2$ were grown out of a self-flux using conventional high-temperature solution growth techniques.[1] The doping level x was determined using wavelength dispersive x-ray spectroscopy in a JEOL JXA-8200 electron microprobe.[1] Long range antiferromagnetism was observed below a transition temperature $T_N(x)$ up to $x \sim 0.06$. Superconductivity appears around $x_{\text{on}} = 0.038$ and vanishes between $0.135 < x_{\text{off}} \leqslant 0.166$ (see Fig. 4).[7] The ARPES measurements were performed at beamline 10.0.1 of the Advanced Light Source (ALS), Berkeley, California, using a Scienta R4000 electron analyzer. Vacuum conditions were better than 3×10^{-11} Torr. The energy resolution was set at $\sim$25 meV. All samples were cleaved *in situ* yielding mirror-like, fresh *a-b* surfaces. High symmetry points were defined the same way as in Ref. 8. TEP measurements were made as described in Ref. 10.

Figure 1 shows the ARPES Fermi maps and corresponding band dispersion data for three different doping levels of Ba(Fe$_{1-x}$Co$_x$)$_2$As$_2$. The incident photon energy is $h\nu = 35$ eV, corresponding to $k_z \simeq 2\pi/c$, the upper edge of the first Brillouin zone (Z).[15] From data in Fig. 1 it is clear that, as electron doping initially increases, the Fermi contours around Z shrink in size. At $x = 0.166$, the edge of the SC dome, the Z pocket shrinks to almost a single point, meaning
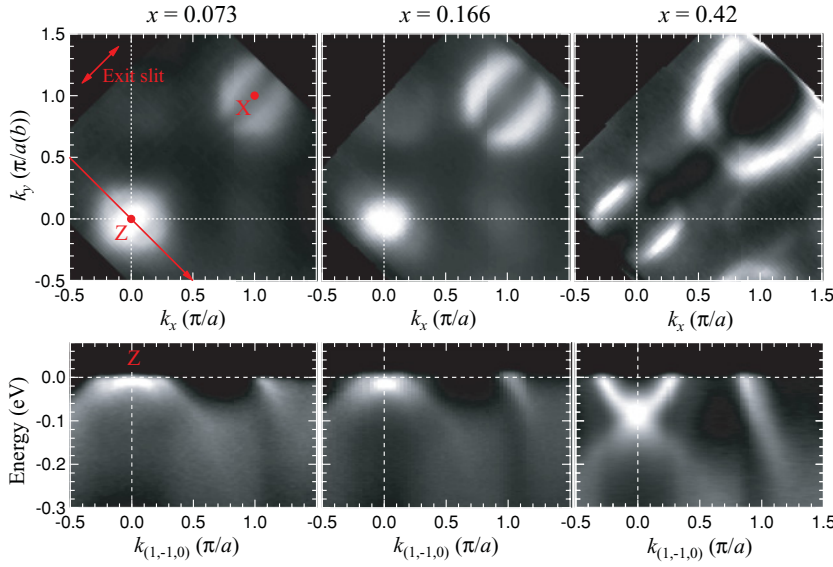
FIG. 1. (Color online) Fermi maps and band dispersion around the upper zone edge Z of Ba(Fe$_{1-x}$Co$_x$)$_2$As$_2$ for $x = 0.073$ (optimal doping), $x = 0.166$ (edge of SC dome), and $x = 0.42$. Upper row: Fermi mappings for the three doping levels, taken with incident photon energy $h\nu = 35$ eV at temperature $T = 20$ K. Red arrows show the exit slit direction of the hemispheric analyzer and the cutting direction of the band dispersion maps (lower row). The same direction is also used in Fig. 2. Note that the X points marked in these figures have slightly lower k_z values than the Z points.

a complete vanishing of the hole pocket. This observation is consistent with the data in Refs. 8, 16, and 17. As x increases, the Z pocket expands again, yielding a diamond shape at $x = 0.42$. Band dispersion clearly reveals that this "diamond" is electron-like. Such an electron pocket is not predicted by band structure calculations.[4] The X pocket, on the other hand, keeps expanding from $x = 0.073$ to $x = 0.42$, and it remains electron-like. The central message of this figure is that the Z pocket undergoes a drastic topological change from hole-like to electron-like at roughly the doping level

where superconductivity vanishes. Based on this observation we perform two independent data analysis procedures with finer doping steps to further pinpoint the doping level of the Lifshitz transition.

First, to obtain a more accurate value for x_2, we extract the energies for the hole band top and the electron band bottom at the zone center, and examine them as a function of cobalt doping. As shown in Fig. 2, we plot the band dispersion maps along the same direction as in Fig. 1 for eight different doping levels ranging from $x = 0.10$ to $x = 0.42$, and use the energy
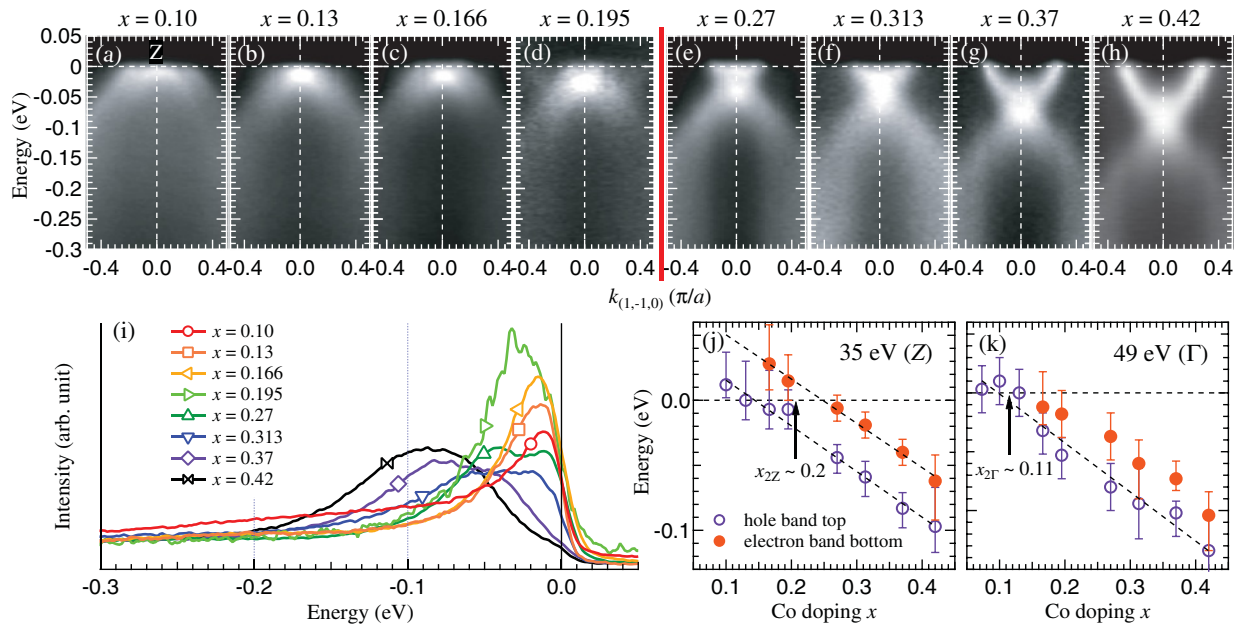

FIG. 2. (Color online) Band location analysis for the Lifshitz transitions. (a)–(h): Band dispersion maps along the direction shown in Fig. 1 for eight different doping levels at $T = 20$ K. All data are taken with 35-eV photons. The red vertical line marks $0.195 < x_{2Z} < 0.27$. (i) Energy distribution curve (EDC) at Z for each doping level. (j) and (k) Evolution of binding energy for the top of the hole band and the bottom of the electron band at the zone center with respect to cobalt doping. x_{2Z} and $x_{2\Gamma}$ are defined as the midpoint between the two doping levels at which the electron and hole band evolves above μ. Data are extracted from ARPES intensity maps taken with (j) 35-eV and (k) 49-eV photons, corresponding to k_z values of Z and Γ, respectively. For $x > 0.195$, data points in (k) are extracted from the EDC's at (i) by fitting with two Lorentzian functions. For $x \leqslant 0.195$, a parabolic function is fitted to the momentum distribution curve (MDC) peak positions of the outer hole band in (a)–(d) for extracting the top of the band above μ. Raw data for extracting panel (k) are not shown.

distribution curves (EDC's) in Fig. 2(i) to see that both the hole band and the electron band shift to higher binding energies as x increases. The shape of these bands remains the same during the process. There is a small gap (~40 meV) between these two bands. At $0.195 < x < 0.27$ the bottom of the electron band moves above the chemical potential, as revealed in Fig. 2(j), where energies of the top of the hole band are extracted from Fig. 2(a)–2(h). At a lower doping level the top of the hole pocket also moves above μ. Figures 2(a)–2(j) illustrate that at the Z point of the Brillouin zone, the Lifshitz transition takes place between $0.195 < x_{2Z} < 0.27$, higher than $x_{off} \sim 0.15$. We observe also from Fig. 2 that, among the three Γ hole pockets resolved by ARPES,[18] the vanishing of the outermost Γ pocket has a much closer relation to the disappearance of superconductivity. One supporting observation is that the strong pairing strength switches to the outer hole pocket in Ba(Fe$_{1-x}$Co$_x$)$_2$As$_2$ (Ref. 13).

The intrinsic three dimensionality of the electronic structure[19,20] results in different x_2 values for different k_z. In Fig. 2(k) we investigate this effect by performing the same analysis on the data taken with 49 eV photons (raw data not shown). This incident photon energy corresponds to $k_z \simeq 0$, the central point of the Brillouin zone (Γ). We see that indeed the Lifshitz transition shifts to $x_{2\Gamma} \sim 0.11$. This observation also supports the theoretical prediction that three dimensionality of the Fermi surface leads to a more gradual decrease of T_c in the overdoped side.[12]

In Fig. 3 we perform a pocket size analysis at Z to further pinpoint x_2. This second procedure is independent from the above energy extraction method. To do this we first find the Z-pocket location for all doping levels studied (ranging from $x = 0.073$ to $x = 0.42$) by fitting the momentum distribution curves (MDC's) at the chemical potential with several Lorenzian functions. From Fig. 3(a) we see a clear evolution of the Z-pocket size with doping. As x increases, the hole pocket shrinks in size up to $x = 0.195$. Above this doping an electron pocket appears and increases in size up to the highest doping measured. As seen in Fig. 3(b), both the hole and electron pocket size evolve in a linear fashion, a signature of the validness of the rigid band-shifting scenario,[21] and of the pockets being paraboloids in shape. The crossover takes place around $x = 0.2$. This Lifshitz transition is best visualized in Fig. 3(c), where data in Fig. 3(a) are plotted against the cobalt doping x as a third dimension. This figure reveals that as cobalt concentration increases, the Fermi sea level rises and the Z hole bands gradually drop below it. At $x \sim 0.2$ the total occupation of the outer hole band marks the Lifshitz transition. Beyond this point the Z pocket becomes electron-like, and superconductivity vanishes.

Figure 4 summarizes our systematic ARPES survey on the Fermi surface topology of Ba(Fe$_{1-x}$Co$_x$)$_2$As$_2$ for $0 \leqslant x \leqslant 0.42$ and compares it with TEP data over the same doping range. The most important finding of this study is that the low- and high-doping onset of the SC region likely link to topological changes of the Fermi surface. The first Lifshitz transition at the low doping onset of superconductivity is described in detail in Refs. 8 and 10. The second and third Lifshitz transitions occur for $0.11 \lesssim x \lesssim 0.2$ and likely correspond to the high doping offset of superconductivity. $x_{2\Gamma} \simeq 0.11$ corresponds to the doping
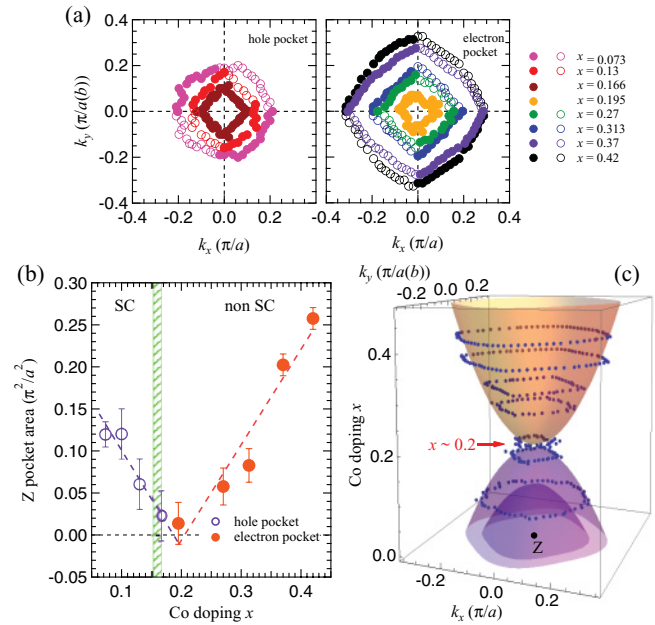

FIG. 3. (Color online) Pocket size analysis for the Lifshitz transition at upper zone boundary Z. (a) Z-pocket extraction for eight doping levels, done by fitting the MDC's at the chemical potential with several Lorenzian functions. Positions of hollow circles are symmetrized from experimental data points (solid circles), proposing the band positions where ARPES intensity is suppressed by the transition matrix element. (b) Evolution of Z-pocket area with cobalt doping. Green shaded area indicates the boundary of the SC dome. (c) Visualization of the Lifshitz transition. Data in (a) are plotted against the cobalt doping x as a third dimension. Shaded areas are approximate size and shape of the pockets. Panels (b) and (c) show a Lifshitz transition at $x_{2Z} \sim 0.2$.

level where the shape of the quasicylindrical outer Γ contour changes to an ellipsoid centering at Z. As doping is increased, this Z ellipsoid shrinks in size until it disappears altogether at $x_{2Z} \simeq 0.2$. On the other hand, superconductivity vanishes at $x_{off} \simeq 0.15$. At $x > 0.2$, the region of the highest doping, the central pocket becomes electron-like, and superconductivity does not exist. It is important to emphasize that the Lifshitz transition need not exactly coincide with SC transition for the two to be related. At the Lifshitz transition, such as in our case, the carriers in a particular Fermi surface sheet vanish from μ completely. If those carriers contributed to a particular property (e.g., SC), one would expect the property itself to disappear at a doping slightly lower than the Lifshitz transition. This is simply because a finite number of electrons is necessary to support macroscopic properties (especially SC). Such a finite number of electrons exists only before the Lifshitz transition takes place. Our TEP data, plotted as $S(x)|_{T=\text{const}}$ for several temperatures in Fig. 4(b), show clear step-like or change-of-slope anomalies at Co concentrations that are in excellent agreement with those at which the Lifshitz transitions were detected by ARPES [Fig. 4(a)]. These results, taken together, confirm extreme sensitivity of TEP to the changes in FS topology.[22]

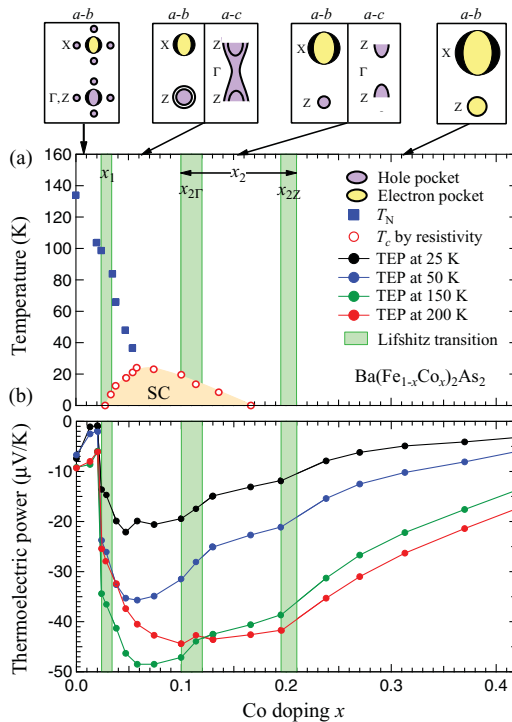Importantly, the above conclusion most likely also applies to other electron-doped 122 systems. We are especially

FIG. 4. (Color online) (a) Location of the known Lifshitz transitions in the phase diagram. T_N and T_c data are taken from Refs. [1] and [8]. Top insets show schematic Fermi surface topology in the *a-b* and *a-c* plane for each region in the phase diagram. (b) Thermoelectric power vs doping for four different temperatures.

only difference being that the corresponding doping levels are roughly one-half of those of the cobalt system. As the phase diagram changes to T vs e, the extra electron count, these two systems match perfectly.

Our findings have important implications on the nature of superconductivity of the pnictides. First, our observation reveals the importance of the underlying Fermi surface topology: a necessary condition for the emergence of superconductivity is likely the existence of the nonreconstructed central hole pockets rather than a perfect nesting condition between the central and corner pockets. Superconductivity is not supported when either one set of these pockets (central or corner) vanishes, changes its carrier nature, or shows considerable reconstruction. Second, our results imply that the suppression of superconductivity on the underdoped side is related to the competition between the AFM and SC phases,[7] whereas on the overdoped side the disappearance of the central hole pocket plays a more important role than the decrease of the pairing interaction magnitude.[12] Our results strongly indicate that the pairing interaction in electron-doped iron pnictides has an interband nature. Electron-doped 122 systems are, therefore, likely candidates of high-temperature superconductors whose superconducting behavior is controlled primarily by the underlying Fermiology. Combining with data from hole-doped 122 compounds,[25] our results point to the implication that Fermiology plays very different roles for the two sides of the phase diagram. This situation is similar to the cases in hole- and electron-doped cuprates and is not surprising given the difference in the respective phase diagrams. A new theoretical approach is necessary to unify the understanding of both families.

interested in $A(Fe_{1-x}Ni_x)_2As_2$ where each nickel atom gives two extra electrons per Fe site compared to one in the cobalt-doped system.[7] There, similar to the cobalt-doped system, the Hall coefficient and thermoelectric power anomaly occurs right at the onset of superconductivity.[8,23] Based on a similar ARPES survey,[24] we indeed find Lifshitz transitions at close proximity to the boundaries of superconductivity, the

[1] N. Ni, M. E. Tillman, J. Q. Yan, A. Kracher, S. T. Hannahs, S. L. Budko, and P. C. Canfield, Phys. Rev. B **78**, 214515 (2008).

[2] J.-H. Chu, J. G. Analytis, C. Kucharczyk, and I. R. Fisher, Phys. Rev. B **79**, 014506 (2009).

[3] F. L. Ning *et al.*, J. Phys. Soc. Jpn. **78**, 013711 (2009).

[4] L. Fang *et al.*, Phys. Rev. B **80**, 140508(R) (2009).

[5] S. Nandi *et al.*, Phys. Rev. Lett. **104**, 057006 (2010).

[6] P. C. Canfield, S. L. Budko, N. Ni, J. Q. Yan, and A. Kracher, Phys. Rev. B **80**, 060501(R) (2009).

[7] P. C. Canfield and S. L. Bud'ko, Annu. Rev. Condens. Matter Phys. **1**, 27 (2010).

[8] C. Liu *et al.*, Nat. Phys. **6**, 419 (2010).

[9] I. M. Lifshitz, Sov. Phys. JETP **11**, 1130 (1960).

[10] E. D. Mun, S. L. Budko, N. Ni, A. N. Thaler, and P. C. Canfield, Phys. Rev. B **80**, 054517 (2009).

[11] D. Innocenti, N. Poccia, A. Ricci, A. Valletta, S. Caprara, A. Perali, and A. Bianconi, Phys. Rev. B **82**, 184528 (2010).

[12] R. M. Fernandes and J. Schmalian, Phys. Rev. B **82**, 014521 (2010).

[13] K. Terashima *et al.*, Proc. Natl. Acad. Sci. USA **106**, 7330 (2009).

[14] S. V. Borisenko *et al.*, Phys. Rev. Lett. **105**, 067002 (2010).

[15] T. Kondo *et al.*, Phys. Rev. B **81**, 060507(R) (2010).

[16] Y. Sekiba *et al.*, New J. Phys. **11**, 025020 (2009).

[17] V. Brouet, M. Marsi, B. Mansart, A. Nicolaou, A. Taleb Ibrahimi, P. LeFevre, F. Bertran, F. Rullier-Albenque, A. Forget, and D. Colson, Phys. Rev. B **80**, 165115 (2009).

[18] T. Sudayama, Y. Wakisaka, K. Takubo, R. Morinaga, T. J. Sato, M. Arita, H. Namatame, M. Taniguchi, and T. Mizokawa, Phys. Rev. Lett. **104**, 177002 (2010).

[19] C. Liu *et al.*, Phys. Rev. Lett. **102**, 167004 (2009).

[20] P. Vilmercati *et al.*, Phys. Rev. B **79**, 220503(R) (2009).

[21] M. Neupane *et al.*, Phys. Rev. B **83**, 094522 (2011).

[22] Y. M. Blanter *et al.*, Phys. Rep. **245**, 159 (1994).

[23] N. P. Butch, S. R. Saha, X. H. Zhang, K. Kirshenbaum, R. L. Greene, and J. Paglione, Phys. Rev. B **81**, 024518 (2010).

[24] A. D. Palczewski *et al.* (in preparation).

[25] V. B. Zabolotnyy *et al.*, Nature **457**, 569 (2009).